Actuator disc model using a modified Rhie-Chow/SIMPLE pressure correction algorithm. Comparison with analytical solutions

Pierre-Elouan Réthoré[1,2,3], **Niels N. Sørensen**[1,2]

[1] Wind Energy Department, Risø National Laboratory for Sustainable Energy, DTU - Technical University of Denmark, DK-4000 Roskilde, Denmark
[2] Department of Civil Engineering, Aalborg University, Sohngaardsholmsvej 57, DK-9000 Aalborg, Denmark
[3] pierre-elouan.rethore@risoe.dk

Abstract:

An actuator disc model for the flow solver EllipSys (2D&3D) is proposed. It is based on a correction of the Rhie-Chow algorithm for using discreet body forces in collocated variable finite volume CFD code. It is compared with three cases where an analytical solution is known.
Key words: CFD, acuator disc, Rhie-Chow, SIMPLE, numerical wiggles, wind turbine, wake

Introduction

The flow going through a wind turbine can be modeled using Computational Fluid Dynamics (CFD) by solving the Navier Stokes equations. The influence of the turbine in the equation can be implemented as a body force acting against the flow. The Navier Stokes equations are essentially composed of velocity terms, of pressure gradient terms and of body forces. When discretized over a mesh using a finite volume method, if the pressure and velocity terms are represented at the same place, a decoupling might occur that can lead to numerical oscillations of the pressure (or pressure wiggles). One way of dealing with this issue is to keep the velocities at the cell faces and the pressure terms at the cell centers, so that the pressure gradient terms, derived from them, are located at the same place as the velocity terms (e.g. the cell centers). This method is called the staggered grid method. The other standard way is to keep the pressure and velocity terms at the cell centers (known as the collocated variable method), and uses a special treatment of the pressure, to avoid the pressure/velocity decoupling. This method, which was first introduced by Rhie-Chow [1], was never intended to take care of the pressure/velocity decoupling introduced by inputting a sudden pressure jumps, or discreet body forces. EllipSys, the in-house curvilinear CFD code designed at Risø National Laboratory for Sustainable Energy (Risø-DTU) [2] and the Fluid Mechanics department of the Technical University of Denmark (MEK-DTU) [3] is based on a collocated variable arrangement using the Rhie-Chow pressure correction algorithm. Discreet body forces are, in the present context, used in order to model the influence of wind turbines on the flow. In order to overcome the pressure wiggles introduced by discreet body forces, one approach is to smooth the body forces out by using a Gaussian distribution instead of a Dirac delta distribution [4]. This method requires that the pressure jump is made over several cells which can become computationally expensive on large problem like simulating a wind turbine farm. In order to save computational time, a modification of the Rhie-Chow algorithm is proposed to treat the special case of discreet pressure jumps.
In the present paper, an algorithm to discretize an actuator disc over a mesh is briefly introduced. Secondly, the problem of the pressure wiggles is presented for a 1D example of a regular Cartesian mesh with a special case of uniform velocity over the domain. The proposed algorithm is then described in the context of the curvilinear CFD code EllipSys3D. For the sake of clarity, the same notations used in

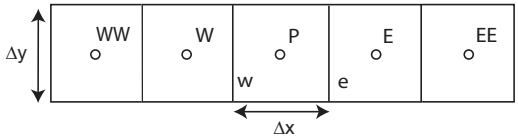

Figure 1: 1D mesh

the original thesis describing EllipSys are used (see Sørensen [2]). Finally three different test cases, for which an analytical solution is known, are presented and compared with Ellipsys results.

1 Description of the algorithm

1.1 Force allocation

The basic idea of the force allocation algorithm used is to, first, search for all the cells which are crossed by the disc. Then, in order to determine the equivalent body force that will be allocated to the cell, to calculate the intersectional surface between the disc and each cell, and to integrate the force distribution of the actuator disc over it. Finally, to apply the pressure jump correction, described in the following section, to redistribute the forces over the neighboring cells, and to derive the corresponding cell faces pressure jumps. The Navier Stokes equations are then solved using the body forces in the momentum equation, and using the pressure jumps in the Rhie-Chow algorithm.

1.2 Pressure jump correction

In order to understand the necessity of the the pressure jump correction, a simple 1D case, with uniform velocity flow is used. Based on this example, the principle of the Rhie-Chow algorithm is briefly introduced. Then, pressure wiggles are shown to be present when discreet body forces are applied. Finally, the basic idea behind the pressure jump correction is presented, and its application to the CFD code EllipSys is described.

Origin of pressure wiggles

The 1D Navier Stokes equations can be written as

$$\frac{\partial \rho U}{\partial t} + \frac{\partial \rho U U}{\partial x} = -\frac{\partial P}{\partial x} + \frac{\partial}{\partial x}\left(\mu \frac{\partial U}{\partial x}\right) + F, \tag{1}$$

where F is a volumic force [N/m^3].

In order to have an equation for the pressure, the Continuity equation is used

$$\frac{\partial \rho U}{\partial x} = 0. \tag{2}$$

In the finite volume formulation, derivatives can be discretized by integrating them over a control volumes. Using a CDS scheme over the 1D mesh presented in Figure 1, the following rules can be applied.

$$\int_P \frac{\partial \Psi}{\partial x} dxdy = (\Psi_e - \Psi_w)\,\Delta y = (\Psi_E - \Psi_W)\,\frac{\Delta y}{2}, \tag{3}$$

$$\begin{aligned} \int_P \frac{\partial \Psi \Psi^*}{\partial x} dxdy &= (\Psi_e \Psi_e^* - \Psi_w \Psi_w^*)\,\Delta y \\ &= (\Psi_E(\Psi_E^* + \Psi_P^*) - \Psi_W(\Psi_W^* + \Psi_P^*) + \Psi_P(\Psi_E^* - \Psi_W^*))\,\frac{\Delta y}{4}, \end{aligned} \tag{4}$$

$$\text{and} \quad \int_P \frac{\partial}{\partial x}\left(\frac{\partial \Psi}{\partial x}\right) dxdy = \left[\left(\frac{\partial \Psi}{\partial x}\right)_e - \left(\frac{\partial \Psi}{\partial x}\right)_w\right] \Delta y = (\Psi_W + \Psi_E - 2\Psi_P)\,\frac{\Delta y}{\Delta x}. \tag{5}$$

where the * indicates that the term is known from a previous time step.
Applying these rules on the Continuity equation (2) gives

$$\Delta y \left(\rho U_e - \rho U_w\right) = 0, \tag{6}$$

which therefore leads to a second relationship,

$$U_W = U_E. \tag{7}$$

Assuming a steady flow and therefore dropping the unsteady term of Equation (1) gives

$$\rho \left[\left(UU^*\right)_e - \left(UU^*\right)_w\right] \frac{\Delta y}{4} = \left(P_W - P_E\right) \frac{\Delta y}{2} + \mu \left(U_W + U_E - 2U_P\right) \frac{\Delta y}{\Delta x} + F_P \Delta x \Delta y. \tag{8}$$

Equation (8) can be rewritten into a general formulation by linearizing and assuming that one of the U's is known in the convective term (UU term)

$$A_P U_P = \sum_P A_P^{nb} U_{nb} + \left(P_W - P_E\right) \frac{\Delta y}{2} + F_P \Delta x \Delta y, \tag{9}$$

with $nb \in (W, E)$, and

$$A_P^W = \mu \frac{\Delta y}{\Delta x} + \rho \frac{\Delta y}{4} (U_W^* + U_P^*), \quad A_P^E = \mu \frac{\Delta y}{\Delta x} - \rho \frac{\Delta y}{4} (U_E^* + U_P^*),$$
$$\text{and} \quad A_P = 2\mu \frac{\Delta y}{\Delta x} + \rho \frac{\Delta y}{4} (U_E^* - U_W^*). \tag{10}$$

Note that Continuity states that $\rho \Delta y U_W = \rho \Delta y U_E$, and so therefore $A_P = A_P^W + A_P^E$.

The cell center velocity obtained from the Navier Stokes equations (9) can be interpolated, using the midpoint rule, at the cell face in order to apply the Continuity

$$U_e = \frac{1}{2} \left(U_P + U_E\right). \tag{11}$$

A simple case can be applied, where the velocity is assumed to be uniform in the domain (i.e. $U_{WW} = U_W = U_P = U_E = U_{EE}$). Combined with the assumption of a regular Cartesian mesh, all the velocity terms and coefficients A_*^* are eventually canceling each other. Inserting Equation (9) into Equation (7) then gives

$$\begin{aligned} \left(P_{WW} - P_P\right) \frac{\Delta y}{2} + F_W \Delta x \Delta y &= \left(P_P - P_{EE}\right) \frac{\Delta y}{2} + F_E \Delta x \Delta y \\ P_{WW} - 2P_P + P_{EE} &= \left(F_E - F_W\right) \Delta x. \end{aligned} \tag{12}$$

If there are no body forces in the domain, the relationship between the pressure at each cell becomes

$$P_P = \frac{1}{2} \left(P_{WW} + P_{EE}\right). \tag{13}$$

As the pressure of a cell is not dependent of its direct neighboring cells pressure, this relationship can be satisfied by a pressure wiggle solution (e.g. 2-0-2-0-2...)

The Rhie-Chow algorithm

The Rhie-Chow algorithm is adressing this issue by separating the pressure terms from the rest of the momentum terms, when the face velocities are derived. Instead of interpolating the pressure gradient at the cell faces using the pressure gradients at the cells center, they are directly derived from the pressure at the closest cells center.

$$U_e = \frac{1}{2} \left(\widetilde{U_P} + \widetilde{U_E}\right) + \frac{\Delta y}{A_e} \left(P_P - P_E\right), \tag{14}$$

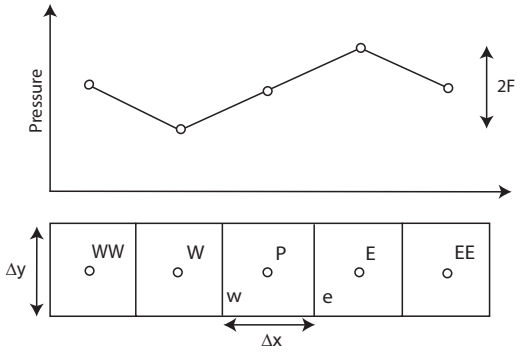

Figure 2: Pressure jump with wiggles

where

$$\widetilde{U_P} = \frac{1}{A_P}\left(\sum_P A_P^{nb} U_{nb} + F_P \Delta x \Delta y\right), \quad \text{and} \quad A_e = \frac{1}{2}\left(A_P + A_E\right). \tag{15}$$

Inserting Equation (14) into the Continuity Equation (2) then brings a different relation

$$\frac{1}{2}\left(\widetilde{U_E} - \widetilde{U_W}\right) + \frac{\Delta y}{A_e}\left(P_P - P_E\right) - \frac{\Delta y}{A_w}\left(P_W - P_P\right) = 0. \tag{16}$$

Applying the same simple case of uniform velocity in the entire domain, with a regular Cartesian mesh, all the velocity terms cancel each other, which brings a relationship between the pressure and the body forces

$$\frac{1}{2}\left(F_E - F_W\right)\Delta x \Delta y + \Delta y\left(2P_P - P_W - P_E\right) = 0. \tag{17}$$

If there are no body forces in the domain, then the pressure in the cell P is related with its direct neighboring cells pressure.

$$P_P = \frac{1}{2}\left(P_W + P_E\right). \tag{18}$$

In this case, the oscillations pressure field is not a solution.

Applying a discreet force or a pressure jump

However, if there is a discreet force F_P applied in the cell P, already from Equation (9), there is a problem. If the velocity is the same over the domain, then all the velocity terms are canceling each other which gives a relationship between the body force and the pressure.

$$P_E - P_W = 2F_P \Delta x. \tag{19}$$

Similarly, applying Equation (**??**) on the cell W and E shows that there is a pressure wiggle solution

$$P_P - P_{WW} = 2F_W \Delta x = 0 \quad \text{and} \quad P_{EE} - P_P = 2F_E \Delta x = 0. \tag{20}$$

So even using the Rhie-Chow correction, applying a sudden pressure jump into this scheme causes the appearance of numerical pressure wiggles (see Figure 2).

Basic idea of the modification

In order to correctly handle discreet forces in the Navier Stokes and the Continuity equations, the forces are defined at the face of the cells in the same way the pressure gradient terms are. The body force in the cell P is splitted into two pressure jumps: one on the west face P_w^j and one on the east face P_e^j respectively. Equation (9) can then be rewritten as

$$A_P U_P = \sum_P A_P^{nb} U_{nb} + \left(P_W - P_E\right)\frac{\Delta y}{2} + \left(P_w^j + P_e^j\right)\frac{\Delta y}{2}. \tag{21}$$

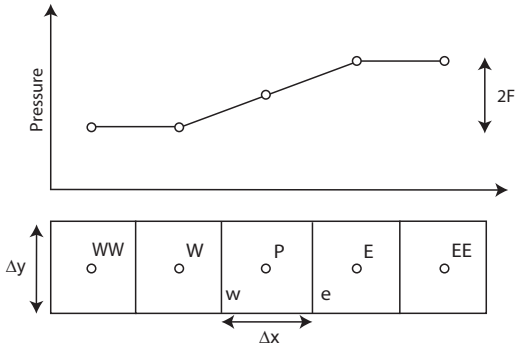

Figure 3: Pressure jump without wiggles

The pressure jumps are then treated in the same way as the pressure gradients during the derivation of the face velocity

$$U_e = \frac{1}{2}\left(\overline{U_P} + \overline{U_E}\right) + \frac{\Delta y}{A_e}\left(P_P - P_E\right) + \frac{P_e^j}{A_e}\Delta y, \tag{22}$$

where

$$\overline{U_P} = \sum_P A_P^{nb} U_{nb}, \quad \text{and} \quad A_e = \frac{1}{2}\left(A_P + A_E\right). \tag{23}$$

The Continuity equation (6) is then giving

$$\frac{1}{2}\left(\overline{U_E} - \overline{U_W}\right) + \frac{\Delta y}{A_e}\left(P_P - P_E\right) - \frac{\Delta y}{A_w}\left(P_W - P_P\right) + \frac{\Delta y}{A_e}P_e^j - \frac{\Delta y}{A_w}P_w^j = 0. \tag{24}$$

Applying the same simple case (uniform velocity and regular Cartesian mesh) brings a relationship between the pressure and the body forces. The Continuity, in Equation (24), then gives

$$P_W + P_E - 2P_P = P_e^j - P_w^j. \tag{25}$$

Furthermore, by canceling the velocity terms, Equation (21) gives

$$P_E - P_W = P_w^j + P_e^j. \tag{26}$$

Finally, combining Equation (25) and (26) gives

$$P_P - P_W = P_w^j \quad \text{and} \quad P_E - P_P = P_e^j, \tag{27}$$

which is the correct result without pressure wiggles (see Figure 3).

Implementation in EllipSys

The SIMPLE algorithm [5] of EllipSys is using the predicted velocity, obtained from the Navier Stokes equations, in order to find the pressure, through the Continuity equation. This pressure is used to correct the predicted velocity so that it complies with the Continuity equation (it is then not complying with the Navier Stokes). The iteration goes on until the velocity converges to a solution that satisfies both the Navier Stokes equations and the Continuity equation.
The Continuity equation can be expressed using the divergence operator

$$\overrightarrow{\nabla} \cdot \overrightarrow{\rho U} = 0. \tag{28}$$

Using the notation of Sørensen [2]-Eq.28 for a curvilinear grid, this equation can be rewritten as

$$\begin{aligned} &\frac{1}{J}\left(\rho U \alpha_{\xi x} + \rho V \alpha_{\xi y} + \rho W \alpha_{\xi z}\right)_\xi \\ &+ \frac{1}{J}\left(\rho U \alpha_{\eta x} + \rho V \alpha_{\eta y} + \rho W \alpha_{\eta z}\right)_\eta \\ &+ \frac{1}{J}\left(\rho U \alpha_{\zeta x} + \rho V \alpha_{\zeta y} + \rho W \alpha_{\zeta z}\right)_\zeta \quad = 0, \end{aligned} \tag{29}$$

where J is the Jacobian of the curvilinear to Cartesian transformation matrix, and the α's are differential areas of the cell faces projected in the Cartesian coordinates. Equation (29) can be written in a more compact way to [2]-Eq.71

$$\frac{1}{J}\left[(C_e - C_w) + (C_n - C_s) + (C_t - C_b)\right] = 0, \tag{30}$$

where $C_e = \rho_e U_e (\alpha_{\xi x})_e + \rho_e V_e (\alpha_{\xi y})_e + \rho_e W_e (\alpha_{\xi z})_e$.

The predicted velocity, derived from the Navier Stokes equations, is composed of implicit terms $(A_{nb}U_{nb})$ and an explicit terms (S_{U-mom}) [2]-Eq.65.

$$U_P = \frac{S_{U-mom} - \sum A_{nb}U_{nb}}{A_{P,U}}, \tag{31}$$

where the explicit terms (S_{U-mom}) contain the cross diffusion terms, the pressure terms and the body forces.

In order to apply the Continuity, it is necessary to find the velocity at the cell faces. The usual collocated approach is to interpolate the velocity U_P at the cell faces. This leads to the pressure wiggles, as explained previously. The idea of the Rhie-Chow algorithm is to separate the pressure gradient terms from the rest, and to directly estimate it at the cell face.

$$\left(\frac{\partial P}{\partial x}\right)_e = \frac{1}{J}\left(\left(\frac{\partial P \alpha_{\xi x}}{\partial \xi}\right)_e + \left(\frac{\partial P \alpha_{\eta x}}{\partial \eta}\right)_e + \left(\frac{\partial P \alpha_{\zeta x}}{\partial \zeta}\right)_e\right). \tag{32}$$

The normal gradients are directly computed using a second order accurate central difference scheme [2]-Eq.42.

$$\left(\frac{\partial P \alpha_{\xi x}}{\partial \xi}\right)_e = (P_E - P_P)(\alpha_{\xi x})_e. \tag{33}$$

The cross-term gradients are computed as the interpolation between two central differences [2]-Eq.43.

$$\left(\frac{\partial P \alpha_{\eta x}}{\partial \eta}\right)_e = \frac{1}{4}[(P_N - P_S) + (P_{NE} - P_{SE})](\alpha_{\eta x})_e \tag{34}$$

$$\left(\frac{\partial P \alpha_{\zeta x}}{\partial \zeta}\right)_e = \frac{1}{4}[(P_T - P_B) + (P_{TE} - P_{BE})](\alpha_{\zeta x})_e. \tag{35}$$

Therefore, instead of interpolating directly (31), the pressure gradient is estimated at the cell faces [2]-Eq.69

$$\begin{aligned} U_e = & \overline{\left(\frac{S_{U-mom} - \sum A_{nb}U_{nb}}{A_{P,U}}\right)_e} + \overline{\left(\frac{1}{A_P}\right)_e}\Big((\alpha_{\xi x})_e(P_E - P_P) \\ & + \frac{1}{4}(\alpha_{\eta x})_e[(P_N - P_S) + (P_{NE} - P_{SE})] \\ & + \frac{1}{4}(\alpha_{\zeta x})_e[(P_T - P_B) + (P_{TE} - P_{BE})]\Big), \end{aligned} \tag{36}$$

where the first term in the Right Hand Side (RHS) is the linear interpolation at the cell face of all the momentum terms except the pressure gradient terms.

In the modification of the Rhie-Chow algorithm, the body forces are also extracted from the momentum terms. They are then transformed into pressure jumps located at each cell faces, in a similar manner as proposed by Mencinger and Zun [6].

$$
\begin{aligned}
U_e \quad = \quad & \overline{\left(\frac{S_{\widetilde{U}-mom} - \sum A_{nb} U_{nb}}{A_{P,U}}\right)_e} + \overline{\left(\frac{1}{A_P}\right)_e} \Big((\alpha_{\xi x})_e (P_E - P_P) \\
& + \frac{1}{4} (\alpha_{\eta x})_e [(P_N - P_S) + (P_{NE} - P_{SE})] \\
& + \frac{1}{4} (\alpha_{\zeta x})_e [(P_T - P_B) + (P_{TE} - P_{BE})] + P^j_{e,\,x} \Big),
\end{aligned} \tag{37}
$$

where $P^j_{e,\,x}$ is the pressure jump at the east cell face in the x direction, and $S_{\widetilde{U}-mom}$ is now the momentum source without the pressure terms and the body forces.

In order to be consistent with the the original body force applied in the cell, the pressure jump needs to satisfy the following property.

$$
\iiint_V \overrightarrow{F}\, dV = \iint_A \overrightarrow{n}\, P^j\, dS. \tag{38}
$$

This relationship can be projected on the Cartesian coordinate system and discretized over the current cell. For the x-direction, this corresponds to

$$
F_{P,\,x}\, V_P = \sum_{nb} n_{nb,\,x}\, S_{nb}\, P^j_{nb,\,x}, \tag{39}
$$

where nb are the neighboring faces, S is the face surface area and V the cell volume, $n_{nb,\,x}$ is the normal vector of the face nb in the x direction.
One solution to this relationship is to weight each faces accordingly to its normal vector and face surface area. The following relationship is complying with Equation (39)

$$
P^j_{nb,\,x} = \frac{F_{P,\,x}\, V_P\, n_{nb,\,x}\, S_{nb}}{\sum_{nb} (n_{nb,\,x}\, S_{nb})^2}. \tag{40}
$$

The pressure jump contributions from the two cells adjacent faces are added up. The final pressure jump can then be used directly in Equation (37)

$$
P^j_{e,\,x} = \frac{F_{P,\,x}\, V_P\, n_{e,\,x}\, S_e}{\sum_{nb,\,P} (n_{nb,\,x}\, S_{nb})^2} + \frac{F_{E,\,x}\, V_E\, n_{e,\,x}\, S_e}{\sum_{nb,\,E} (n_{nb,\,x}\, S_{nb})^2}. \tag{41}
$$

Finally, the forces used in the Navier Stokes equations are recomputed at the cell center using the face pressure jumps and divided by two, so that each neighboring cells carry out the pressure jump equally.

$$
F'_{P,\,x}\, V_P = \frac{1}{2} \sum_{nb} n_{nb,\,x}\, S_{nb}\, P^j_{nb,\,x} \tag{42}
$$

Therefore, the new $F'_{P,\,x}$ is not exactly the same as the original $F_{P,\,x}$. In practice the force has been smeared over the nearest neighboring cells, so that the jump of pressure, corresponding to the body force, is occurring at the cell faces.
The new face velocity can be used in the face mass flux coefficients from Equation (30), which is then used to compute the pressure and to correct the velocity, in order to satisfy Continuity.

2 Analytical validation

In order to study the validity of the actuator disc model, and the impact of the pressure jump correction, three cases, where the analytical formula are known, are compared with the model, with and without the pressure jump correction. The model is both implemented in 2D and in 3D. As the results of the 2D code and the 3D code are giving similar results within the convergence precision required, only the 3D results are presented here.

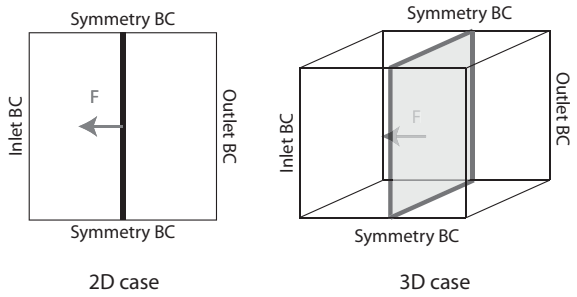

Figure 4: 2D infinite line

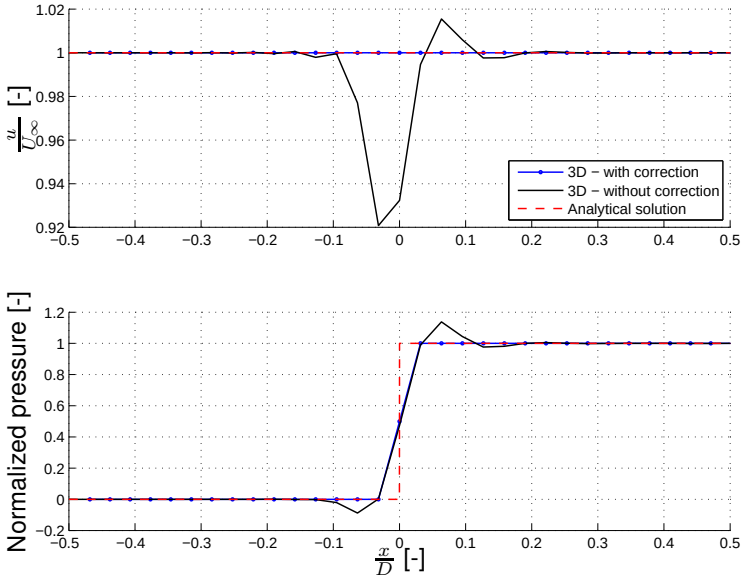

Figure 5: Infinite line/plane case

2.1 2D Infinite line and 3D Infinite plan

The first case studied is a channel flow similar to the example presented in the previous sections. The boundary conditions are taken to be symmetric on the side, so that no expansion is possible. An homogenous force, opposed to the flow direction, is applied along a line (in 2D) or a plane (in 3D) (see Figure 4. This setup insures that the flow direction remains 1D and constant because of Continuity. Only the pressure is expected to vary along the domain, increasing in a discreet manner from one side to the other of the line/plane, as it was described in the previous sections.

The results from the EllipSys (see Figure 5) are in agreement with the theory presented in the previous sections. Using the uncorrected algorithm, the pressure presents some wiggles, visibly damped after 5-6 cells both before and after the jump. The velocity is also presenting wiggles on the same cells where the pressure is fluctuating.
Using the corrected algorithm, the pressure follows a clean jump carried over three cells, in good agreement with the analytical solution. There are no visible wiggles on the pressure, nor on the velocity results.

2.2 2D actuator strip and 3D actuator infinite ribbon

The second case is a 2D actuator strip under a rectangular inflow profile. In order to model it in 3D, the top and bottom faces of the domain are taken as symmetric boundary condition, while the north

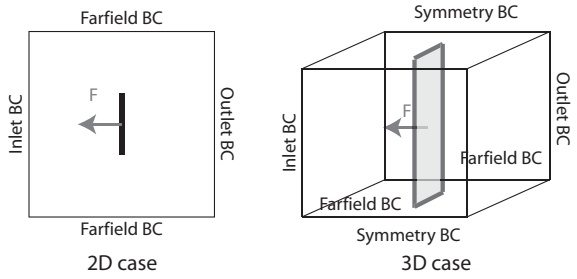

Figure 6: 2D actuator strip

and south faces are taken as farfield boundary conditions. The actuator strip is then represented as an infinitely long ribbon of homogenous force going through the domain from top to bottom (see Figure 6).

The analytical solution for lightly loaded actuator strip, derived by Madsen [7], is used as followed.

$$p(x, y, \Delta p, R) = \frac{\Delta p}{2\pi}\left(\tan^{-1}\left(\frac{R-y}{x}\right) + \tan^{-1}\left(\frac{R+y}{x}\right)\right) \tag{43}$$

$$v_x(x, y, \Delta p, R) = u_\infty - \frac{p(x, y, \theta, \Delta p, R)}{\rho u_\infty} - \underbrace{\frac{\Delta p}{\rho u_\infty}}_{\text{only in the wake}} \tag{44}$$

The assumptions made to derive this equation are only valid for a very lightly loaded actuator disc ($C_T \ll 1$). For a very lightly loaded actuator strip ($C_T = 0.01$), the numerical result, using the correction, is in good agreement to the analytical solution (see Figure 7). Similarly to the previous case, the numerical result without the correction is presenting quite important velocity and pressure wiggles in the axial direction, both before and after the position of the actuator strip. However, there are no visible wiggles in the radial direction.

2.3 3D actuator disc with axis symmetry

Finally the case of an actuator disc in 3D is studied. In order to model the flow appropriately, the boundary condition on the side faces (south, north, top, bottom) are all taken as farfield (see Figure 8).

The analytical solution for an axis symmetric lightly loaded actuator disc in cylindrical coordinates, derived by Koning [8], can be numerically integrated using the following equations.

$$p(x, r, \theta, \Delta p, R) = \frac{\Delta p}{4\pi}\int_0^R \int_0^{2\pi} \frac{r' x}{\left[r'^2 + r^2 + x^2 - 2r' r\cos\left(\theta' - \theta\right)\right]^{3/2}} dr' d\theta \tag{45}$$

$$v_x(x, r, \theta, \Delta p, R) = u_\infty - \frac{p(x, r, \theta, \Delta p, R)}{\rho u_\infty} - \underbrace{\frac{\Delta p}{\rho u_\infty}}_{\text{only in the wake}} \tag{46}$$

The assumptions made to derive this equation are only valid for a very lightly loaded actuator disc ($C_T \ll 1$). For a very lightly loaded actuator disc ($C_T = 0.01$), the numerical result, using the correction, is also in good agreement to the analytical solution. The behavior of the numerical result, without the correction, looks very similar to the previous actuator strip case. Velocity and pressure wiggles are clearly visible both before and after the position of the body forces, in the axial direction, but not in the radial direction.
It is interesting to note that the wiggles do not seem to affect the overall solution. They only give an error at the local position of the actuator disc. It is nonetheless rather interesting to obtain a correct velocity and pressure at the actuator disc position, as this information can be used, for example, to determine the energy extraction of the wind turbine modeled by the actuator disc.
For a more heavily loaded actuator disc ($C_T = 0.89$), a similar convergence is achievable, but it is irrelevant to compare it with the analytical solution.

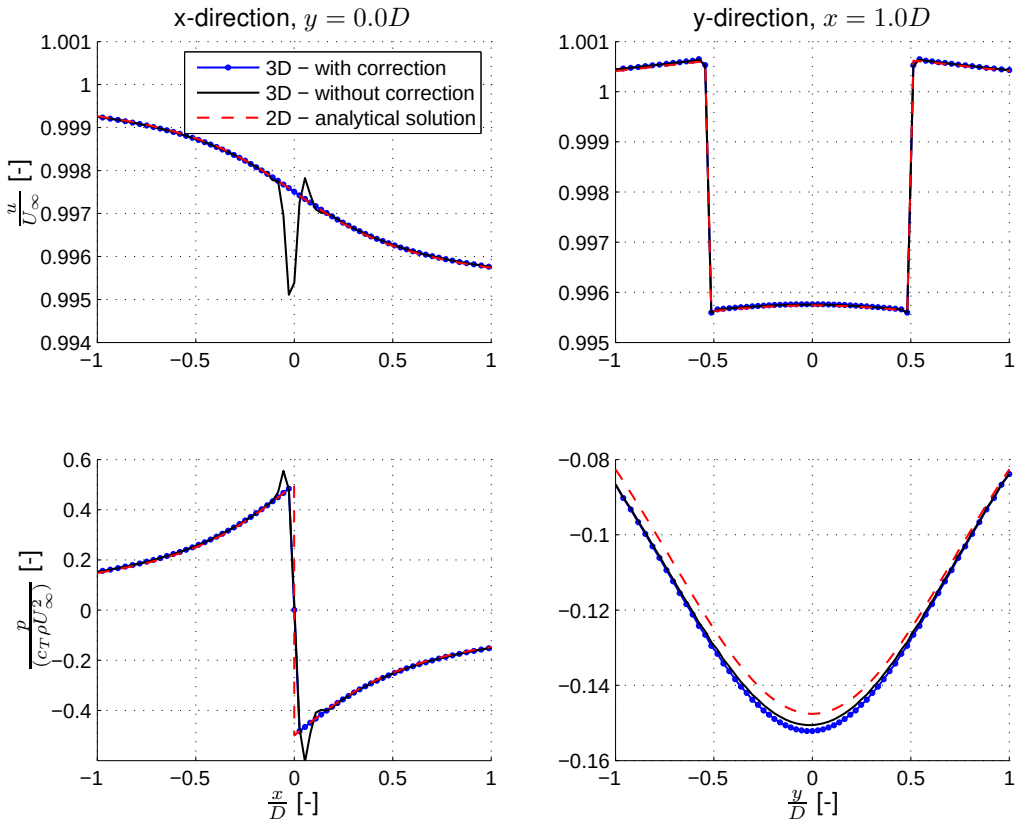

Figure 7: Infinitely long actuator ribbon (3D) compared with a 2D analytical solution for an actuator strip

3 Conclusion

An actuator disc model using a correction of the Rhie-Chow algorithm for the usage of discreet body forces is presented. The corrected algorithm show a clear improvement of the solution around the location where the body forces are applied. This alternative way of treating body forces as pressure jump can reduce significantly the number of cells needed to model a pressure jump. In the present research context, this can potentially lead to cheaper modeling of wind turbine near wake region, and therefore opening the possibility to model larger wind farms. The results from the actuator disc model show a good agreement with analytical solutions, for some lightly loaded cases.

4 Acknowledgment

The current PhD project is supported by the Danish Public Service Obligation (PSO) research project *Flaskehalse*.

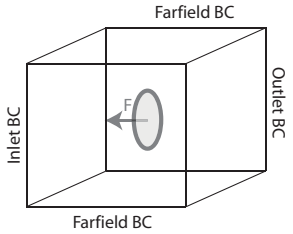

Figure 8: 3D actuator disc

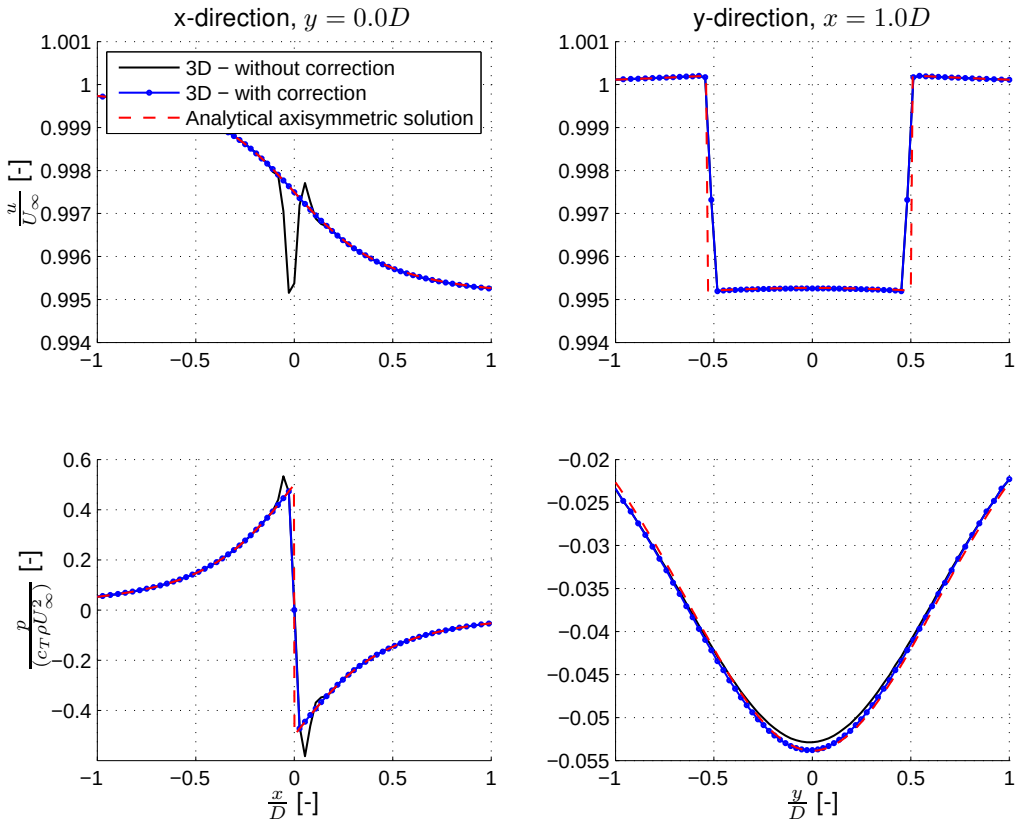

Figure 9: Actuator disc (3D) compared with an analytical axisymmetric solution

References

[1] C.M. Rhie and W.L. Chow. Numerical study of the turbulent fow past an airfoil with trailing edge separation. *AIAA Journal*, 21:1525–1532, 1983.

[2] N.N. Sørensen. *General Purpose Flow Solver Applied to Flow over Hills*. PhD thesis, Technical University of Denmark, 1994.

[3] J.A. Michelsen. Basis3d - a platform for development of multiblock pde solvers. Technical report afm 92-05, Technical University of Denmark, Lyngby, 1992.

[4] R. Mikkelsen. *Actuator Disc Methods Applied to Wind Turbines*. PhD thesis, Technical University of Denmark, Mek dept, 2003.

[5] S.V. Patankar and D.B. Spalding. A calculation procedure for heat, mass and momentum transfer in three-dimensinoal parabolic flows. *Int. J. Heat Mass Transfer*, 15:1787–1972, 1972.

[6] J. Mencinger and I. Zun. On the finite volume discretization of discontinuous body force field on collocated grid: Application to vof method. *Journal of Computational Physics*, 221:524–538, 2007.

[7] H.A. Madsen. Application of actuator surface theory on wind turbines. *IEA R&D WECS, Joint action on Aerodynamics of wind turbines, Lyngby, Denmark*, nov 1988.

[8] C. Koning. *Aerodynamic theory: A general review of progress - Vol.IV. Division M, Influence of the propeller on other parts of the airplane structure, p.366*. Peter Smith, 1976.